

## SIMULATION OF EPITAXIALLY GROWN GRAPHENE ON STEP-SHAPED SiC SURFACE

BARULIN Aleksei, ŠMARHÁK Jiří, VOVES Jan

*Czech Technical University in Prague, Faculty of Electrical Engineering, Czech Republic, EU*  
[smarhjr@fel.cvut.cz](mailto:smarhjr@fel.cvut.cz)

### Abstract

In this study we present calculation of molecular mechanic and electronic transport properties of epitaxially grown graphene on step-shaped SiC substrate. We simulated two types of structural arrangements. The first structure, simulated mainly for purposes of comparison, is planar SiC with graphene bilayer. The second structure is step-shaped SiC with graphene monolayer. We analyzed effects of hydrogenization of the SiC surface and conducted a series of calculations addressing shape of the resulting graphene layers. Finally, we calculated transmission spectrum and I/V curve of resulting structures.

**Keywords:** First principle simulation, SiC, graphene

### 1. INTRODUCTION

The main goal of this study is to predict the structural and electronic properties of graphene nanoribbon-like structure formed on the step-shaped SiC by means of suitable quantum simulation methods. Because of the unique electronic properties, the freestanding graphene nanoribbons are intensively investigated in the last few years. The potential application extends to gas sensors, field effect transistors, spintronics, plasmonics and more. Until recently, there was no possibility to inexpensively produce such structures. By exploiting the different crystallographic planes of SiC, a promising method, which may be used to produce freestanding graphene, was enabled. Graphene is a monolayer material with single-atom thickness composed of hexagonally oriented carbon atoms. It has many interesting properties, depending on its morphology and atomic structure [1]. When infinite graphene crystal becomes finite, surface and boundaries appear, forming atoms at the edges without the third neighbour carbon atom. If the size is of the order of nanometers, graphitic nanostructure exhibits different properties from those which were observed in an infinite layer. Among these graphitic nanostructures are nanoribbons and nanoclusters. Graphene nanoribbons have borders which can exhibit edge states and different electronic, chemical and magnetic properties depending on the size and type of the border. The most studied chiral edge configurations, 0° (armchair) and 30° (zigzag), leads to armchair and zigzag nanoribbons (A-GNRs, Z-GNRs). Z-GNRs exhibit edge states, which are not presented in the armchair case. These edge states are presented as a flat band around the Fermi energy level, but extended along the ribbon's edge. It leads to a metallic nanoribbon if the width is large enough (e.g. > 10 nm). Such flat band leads to a high density of states located at the edges, indicating that they are very reactive sites. Furthermore, Z-GNRs exhibit magnetic properties that are relevant (e.g.) for spintronics [2].

The main problem of graphene nanotubes and nanoribbons are difficulties in the control of the position, radius, chirality and length. It is more desirable to prepare the graphene directly on an insulating substrate then pattern the graphene in areas where it is required via process flow similar to one used for silicon-on-insulator devices. A graphene grown on insulator allows integration of large scale circuits, not just individual devices. A process of generating graphene on insulator, or more specifically multilayer epitaxial graphene (MEG) on SiC (MEG/SiC), has been developed by the high temperature sublimation of silicon from SiC [3]. Growing thick graphite samples on SiC has been a well-known process for many years until the thickness was decreased to a few layers, and a full characterization of the high quality graphene sample carried out. The growth of epitaxial graphene on SiC is based on thermal decomposition of the SiC substrate. E-beam heating as well as resistive heating is used, but no difference seems to arise from the different heating methods. In order to avoid

contamination the heating is usually performed in ultra-high vacuum (UHV) environment or sometimes with Ar gas. From the molar densities one can calculate that approximately three bilayers of SiC are necessary to set free enough carbon atoms for the formation of one graphene layer. The growth of the graphene can take place on the (001) (silicon-terminated) or (0001) (carbon terminated) faces of 4H-SiC and 6H-SiC wafers. The main difference lies in the sample thickness that one can achieve. In the case of the silicon face, the growth is slow and terminates after relatively short time at high temperatures leading to the rise of very thin samples, down to a monolayer. On the contrary, in the case of the carbon face, the growth does not self-terminate leading to the rise of the relatively thick samples (approximately 5 up to 100 layers) with larger orientation and turbostratic disorder [4].

## 2. THE GRAPHENE/SiC INTERFACE MODEL

Because of the relation between graphene and SiC lattice constants, there is a large number of possible orientations of graphene. One structure of particular relevance is the  $(6\sqrt{3} \times 6\sqrt{3})R30$  structure. Note the high symmetry points of the graphene lattice relative to the SiC. There are points where either the carbon atom in the graphene layer sits directly above an atom in the SiC layer below, or a SiC atom lies directly below the center of a graphene hexagon. We can define a quasi-unit-cell that is defined by these high symmetry points. For the appropriate  $(6\sqrt{3} \times 6\sqrt{3})R30$  structure the quasi-cell would be a  $(6 \times 6)$  SiC unit cell [5]. The primary cell of this structure is long and it takes long time to proceed one calculation. So this cell is usually artificially decreased. As a result we get simple model of graphene sitting above a relaxed bulk bilayer. Models like these cannot accurately describe the interface layer, but can predict a number of important results. Firstly, the relaxed distance between the last substrate atom and the first graphene layer is larger on the Si-face (about 2.0 Å) than on the C-face. Secondly, the evolution of the band structure with the number of graphene layers can be predicted. The first graphene layer, which is more tightly bounded to the substrate, has a significant distortion of the  $\pi$ -bonds that gives the growth to a gap in the band structure. This first graphene layer shows no evidence of a graphitic electronic nature. The second graphene layer has the linear dispersion at the k-point characteristic of an isolated graphene sheet. Thus, in these calculations, the first graphene layer on both substrates acts as a 'buffer' layer electrically isolating the second graphene layer from the substrate. The third graphene layer shows splitting of the hole and electron states at the k-point stacked graphene bilayer. It is important to realize that, as the graphene forms, the surface of the sample will recede when Si atoms are leaving. The carbon content in a single graphene monolayer is very close to three SiC bilayers (36.5 atoms/nm<sup>2</sup>). The latter constitutes 0.75 nm of the height in its SiC form, whereas the graphene monolayers are spaced by about 0.34 nm from each other and have similar spacing to the SiC (for the C-face) or the  $6\sqrt{3}$  layer (for the Si-face). Thus, for each additional monolayer of graphene, the top surface must recede by about 0.4 nm. So, if graphene thickness is different across the sample, thickness of substrate is different as well. Also, graphene thickness is measured in number of graphene layers, which is discrete number. Assume sample with 1, 2, 3 and 4 monolayers graphene thickness on it. The morphology of the surface of such sample changes: now is covered by step edges. With the flat regions of the surface, steps form irregularly-shaped  $\mu$ m-sized regions, which are separated from neighbouring terraces by step bunches.

If we compare the Si-face and C-face graphene morphologies for a fixed film thickness, we can find that they are very different. But if we compare them at fixed temperatures, the differences become understandable, at approx. 1320°C. The films thickness on the C-face is much greater than for the Si-face (16 vs. 2 ML), but both films display the characteristic ridges associated with strain relaxation. Both surfaces display comparable amount of step bunching. The reason for choosing the thicker film on the C-face is that the (0001) surface and the (0001)/graphene interface have higher energies (are more unstable), respectively, than the (0001) surface and (0001)/graphene interface. Additionally, more defects in the C-face films such as the discontinuities and rotational domain boundaries can lead to easier Si diffusion through the graphene, which will also provoke thicker growth.

When graphene is based on the Si-face in 1 atm of argon, the tendency to grow in a layer-by-layer manner becomes even more pronounced. In that case, it is quite easy to produce a single monolayer extending over order of 10 or 100 of  $\mu\text{m}$  on the surface. As indicated above, the electronic properties of EG on SiC are layer dependent. An important fact is that the buffer layer has an energy gap at  $E_F$ , so transport experiments and valence spectroscopies measure the effect of the graphene layers. The experimental  $E(k)$  is linear, with a characteristic band velocity consistent with the band structure of an ideal monolayer. Close examination of the spectrum reveals a small shift of the energy bands above the Dirac (charge neutrality) point ED relative to the bands below ED. It was ascribed to many-body interactions or to the creation of a small band gap. The parabolic energy bands of layer 2 graphene are apparent, as is the lower energy split-off band. These observations are predicted for bilayer graphene. The small energy gap centered around -350 meV is the result of the interface electric field; it can be driven to zero by balancing the interface field with an electric field contributed by surface adsorbates. Carrier density is also a layer dependent quantity in EG. The charge neutrality point shifts with respect to the Fermi level (zero tunnel bias) for successive EG layers on SiC(0001) [6].

The morphology of epitaxial graphene on SiC is highly influenced by the underlying SiC structure. Steps on substrate can lead to the problem with proper graphene growing without junk effects, but for few-nm steps the graphene lattice is continuous. It is well known fact, that SiC{0001} surfaces exhibit step bunching. Steps which are perpendicular to the directions  $\langle 1100 \rangle$  are strongly favored on (0001). It is perhaps expected that epitaxial graphene growth should proceed first on nanofacets. High temperature annealing causes vertically etched steps (on the order of 10 nm deep) to produce (1-10) facets with a normal that has an angle of  $23^\circ$  with respect to the {0001} direction. Cross sectional, high resolution transmission electron microscopy of the graphene on steps on SiC has shown that the graphene terminates perpendicular to the silicon carbide surface both on the bottom of the step or on the steps themselves. Moreover, these atomic resolution studies further show that the graphene edges are along the zigzag direction, indication that the graphene sidewall ribbons are zigzag ribbons. This is very important when the edge structure determines the electronic properties of the ribbons. In particular, zigzag ribbons are always metallic. In [7] are introduced experimental results of produced graphene structures by using standard lithography methods of producing an etch mask on the surface. Then, the masked surface was subjected to a plasma etch to etch the desired pattern to a predetermined depth into the surface. Then at temperature of about  $1550^\circ\text{C}$ , in about 10 minutes, the monolayer of graphene has been grown over the step. It presents an important step towards the realization of high mobility quasi 1D graphene structures that do not suffer from the strong localization effects observed in conventionally patterned graphene structures. In [8] the possibility of graphene production is also shown and resistivity of graphene was measured. According to experimental data, graphene with length about  $1.6 \mu\text{m}$  and width about 39 nm has resistivity 26.1 k $\Omega$ . Hydrogen can saturate the silicon dangling bonds without a real decoupling of the interface. In these conditions the charge transfer to the graphene layer is reduced and, as a consequence, the carrier concentration decreases and the carrier mobility increases by about a factor of 2 to 5. The treatment is robust against nanofabrication and thermal cycling, from room temperature down to cryogenic temperature [7].

### 3. STRUCTURE AND SIMULATION METHOD

We used the Atomistix ToolKit (ATK) simulation software with Virtual NanoLab (VNL) user environment by QuantumWise [9-11]. In this work we consider two different structures: graphene on step shape SiC substrate and graphene on planar substrate with additional interface graphene layer. All primitive cells were taken from VNL database. We used moissanite (SiC) as a substrate because of its hexagonal crystal system. Because of stochastic behavior of the graphene on SiC, the covalent bonds between layers have no period and after optimization it becomes even worse. The problem is that at the end we will have very long structure with thousands of atoms. To avoid such problem we need to create the device directly from initial bulk and then do all optimization and passivate structure by hydrogen. The distance between the first layer of graphene and SiC substrate is approx. equal to  $1.43 \text{ \AA}$ , this value is given differently in different papers, so the main criteria was

the maximum distance on which we could get covalent bonds between layers. The distance between the first and the second graphene layer is equal to 2.7 Å on this distance.

The next structure we are focused on is graphene on step shape SiC. The main problem here is to save proper structure of SiC and graphene. Because of the different lattice constant, it is very difficult to make sure that structure is periodic in all directions. We have to reduce a number of atoms as much as possible to minimize the time of calculations. So graphene was a little bit stretched. Then the structure was also passivated by hydrogen and optimized by minimization of Brenner potential. In the case with planar structure the minimum max force component was reached is 1.0899 eV/Å, for step structure it is  $3.3424 \times 10^{-4}$  eV/Å.

In order to minimize the time of calculation, we used Extended Hückel method in both cases. We use Cerda.Carbon[graphite] basis with vacuum level -7.36577 eV, Cerda.Hydrogen [C2H4] basis with vacuum level -6.2568 eV and Cerda.Silicon [GW SiC] basis with vacuum level -6.14175 eV, following the QuantumWise manual recommendation. We used k-point sampling:  $n_A = 10$ ,  $n_B = 3$  and  $n_C = 100$  for flat structure and  $n_A = 4$ ,  $n_B = 4$  and  $n_C = 100$  for step structure. We picked these values empirically trying to find compromise between accuracy and computational time. We used FFT2D as a poisson equation solver, which uses periodic boundary conditions in front, back, bottom, top and Dirichlet in left and right. We also need to make sure that periodic condition in top and bottom direction does not affect our structure by extending the cell borders respectively. We calculated transmission spectrum and I/V curve.

#### 4. NUMERICAL RESULTS

The example of results of the molecular mechanic simulation are on the **Figure 1**.

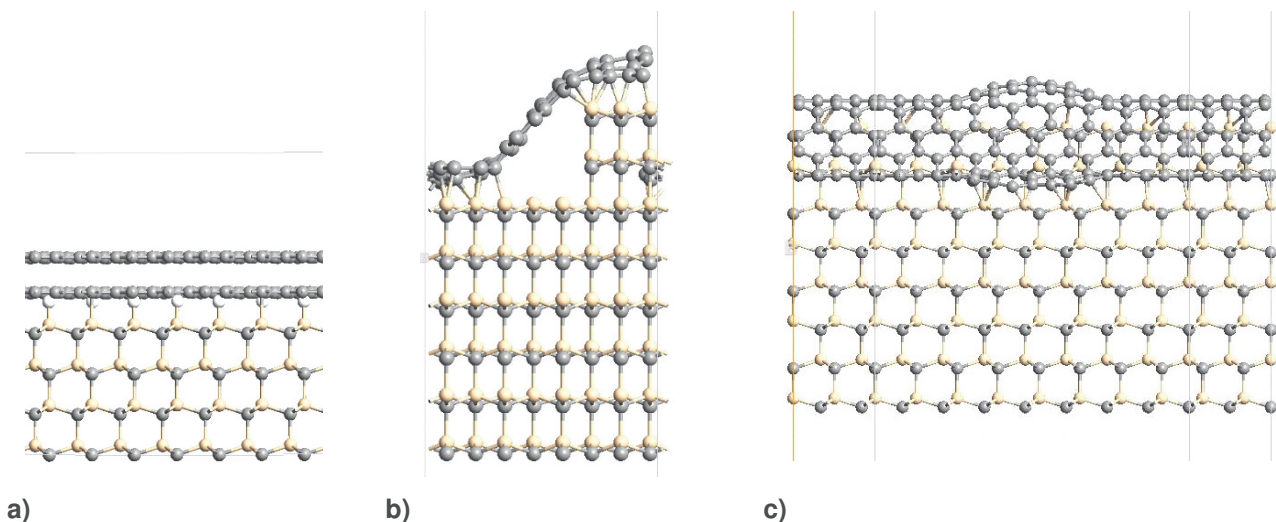
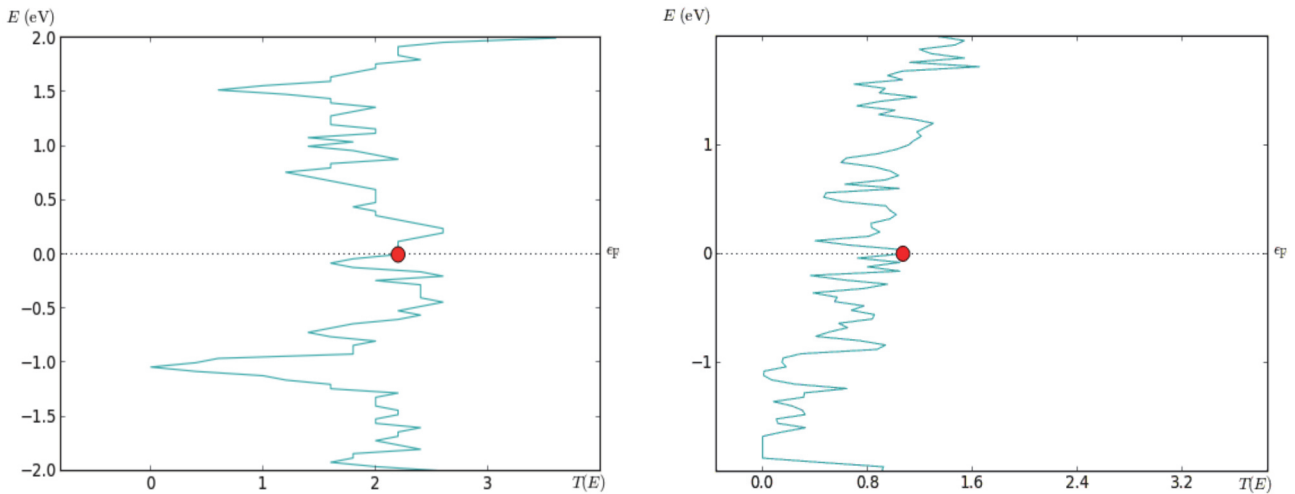


**Figure 1** The result of molecular mechanic simulation of a) bilayer graphene on hydrogenated planar SiC substrate, b, c) step shaped non-hydrogenated non planar SiC substrate (front and side view)

The obtained transmission spectra for the planar and non-planar hydrogenated structures are in the **Figure 2**. As we can see in the **Figure 3**, the coefficient of I/V curve of step-shaped structure is approx. 0.075 S, which is almost twice less than for the flat structure. From the calculated results it can be deduced that SiC is conductive on energies higher than 1 eV. The **Figure 4** describes the base state of electron wave function in the step-shaped non-hydrogenated SiC/graphene interface.



a) b)  
**Figure 2** Transmission spectra for structure with hydrogenated a) planar SiC/bilayer graphene interface, b) step-shaped SiC/graphene interface

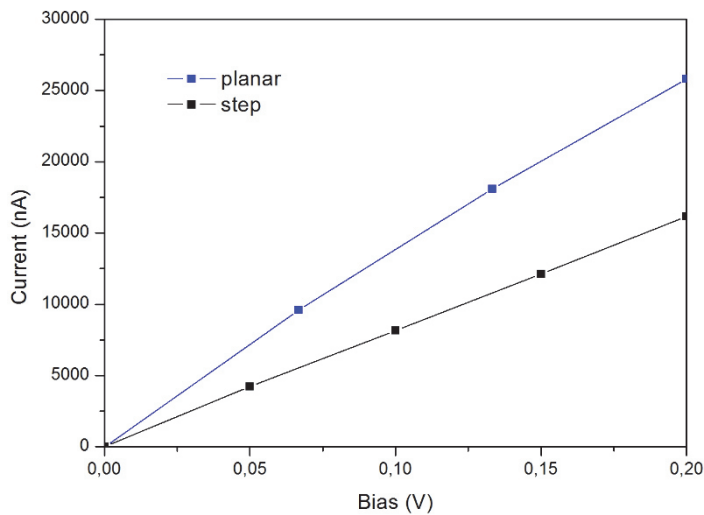


**Figure 3** Comparison of the I/V curves of structure with planar hydrogenated SiC/bilayer graphene interface (blue) and structure with hydrogenated step-shaped SiC/graphene interface (black)

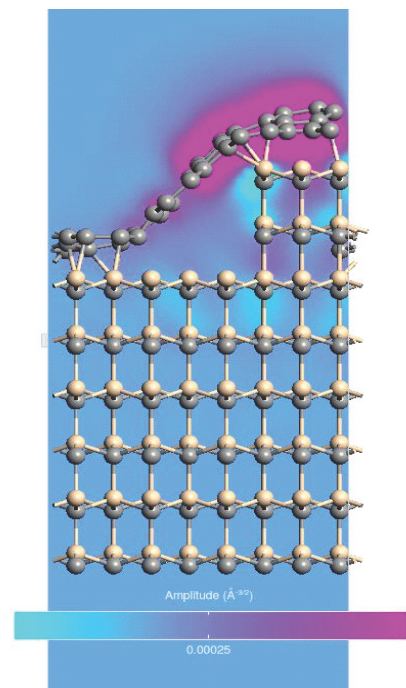


**Figure 4** Base state electron wave function in the structure with step-shaped SiC/graphene interface

## 5. CONCLUSION

Our results were compared with the experimental data. The transmission property was selected to evaluate the accuracy. We can look more precisely at resistivity of the graphene nanoribbon. Our calculation shows that the coefficient of I/V curve of step-shaped structure is approx. 0.075 S, which is almost twice less than for the flat structure. Experimental data from the article [11] gives us a value of 26 kΩ for the graphene sample of

length 1.6  $\mu\text{m}$  and width 39 nm. If we take into account that our step structure model is 1000 times shorter and 20 times narrower, our value of resistance ( $13\Omega$ ) has the same order but is still a bit smaller than the experimental one. The reason is that the collision of electrons with phonons are not taken into account as well as the temperature of environment and other unideal conditions which we can meet in the real case. These data can be used for continuous investigation of graphene on SiC properties.

## ACKNOWLEDGEMENTS

*The paper was supported by the student grant of CTU No. SGS16/089/OHK3/1T/13.*

## REFERENCES

- [1] *Physics and applications of graphene - experiments*, ed. by MIKHAILOV, S., InTech, 2011
- [2] TERRONES, M., BOTELLO-MÉNDEZ, A. R., CAMPOS-DELGADO, J., et al, *Graphene and graphite nanoribbons: Morphology, properties, synthesis, defects and applications*, *Nano Today*, vol. 5, no. 4, pp. 351-372, 2010
- [3] ZHOU, S. Y., GWEON, G.-H., FEDOROV, A. V., FIRST, P. N., DE HEER, W. A. et al, *Substrate-induced bandgap opening in epitaxial graphene*, *Nat. Mater.*, vol. 6, no. 10, pp. 770-5, 2007
- [4] YU, X. Z., HWANG, C. G., JOZWIAK, C. M., KÖHL, A., SCHMID, A. K., LANZARA, A., *New Synthesis Method for the Growth of Epitaxial Graphene*, *Journal of Electron Spectroscopy and Related Phenomena*, vol. 184, pp. 100-106, 2011
- [5] HASS, J., DE HEER, W. A., CONRAD, E. H., *The growth and morphology of epitaxial multilayer graphene*, *J. Phys. Condens. Matter*, vol. 20, no. 32, p. 323202, 2008
- [6] LALMI, B., GIRARD, J. C., PALLECCHI, E., SILLY, M., *Flower-Shaped Domains and Wrinkles in Trilayer Epitaxial Graphene on Silicon Carbide*, *Sci. Rep.*, vol. 4, pp. 225-229, 2014
- [7] HU, Z., RUAN, M., GUO, Z., DONG, R., PALMER, HANKINSON, J., BERGER, C., DE HEER, W.A., *Structured epitaxial graphene: growth and properties*, *J. Phys. D. Appl. Phys.* , vol. 45, p. 154010, 2012
- [8] BARINGHAUS, J., RUAN, M., EDLER, F., et al. *Exceptional ballistic transport in epitaxial graphene nanoribbons*, *Nature*, vol. 506, no. 7488, pp. 349-354, 2014
- [9] Atomistix ToolKit version 12.2, QuantumWise A/S ([www.quantumwise.com](http://www.quantumwise.com)), 2015
- [10] BRANDBYGE, M., MOZOS, J.-L., ORDEJÓN, P., TAYLOR, J., STOKBRO, K., *Density-functional method for nonequilibrium electron transport*, *Phys. Rev.*, vol. B 65, 165401, 2002
- [11] SOLER, J. M., ARTACHO, E., GALE, J. D., GARCÍA, A., JUNQUERA, J., ORDEJÓN, P., SÁNCHEZ-PORTAL, D., J., *The SIESTA method for ab initio order-N materials simulation*, *Phys. Condens. Matter*, vol. 14, p. 2745, 2002